REPORT NO.
UCB/SEMM-90/12

STRUCTURAL ENGINEERING,
MECHANICS AND MATERIALS

A UNIFIED APPROACH TO MIXED FINITE ELEMENT METHODS: APPLICATION TO IN-PLANE PROBLEMS

by

SHMUEL L. WEISSMAN

and

ROBERT L. TAYLOR

JULY 1990

DEPARTMENT OF CIVIL ENGINEERING
UNIVERSITY OF CALIFORNIA
BERKELEY, CALIFORNIA

A UNIFIED APPROACH TO MIXED FINITE ELEMENT METHODS: APPLICATION TO IN-PLANE PROBLEMS

by

Shmuel L. Weissman & Robert L. Taylor

Department of Civil Engineering

University of California at Berkeley

ABSTRACT

A general method to treat internal constraints within the context of mixed finite element methods has been presented in previous work. The underlying idea is to constrain the assumed stress and strain fields to satisfy the homogeneous equilibrium equations in a weak sense and thus, satisfy *a priori* the internal constraints. This method is now applied to generate four-node plane stress/strain elements. For these elements, it is proved that locking at the nearly incompressible limit (plane strain) is avoided at the element level. The proposed elements are shown to yield excellent results on a set of standard problems. Furthermore, excellent stresses are obtained at the element level.

CONTENT

1. INTRODUCTION
   - 1.1 Motivation and objectives
   - 1.2 Background
   - 1.3 Paper overview
2. SUMMARY OF ASSUMED FIELDS GENERATION PROCEDURE
3. PLANE STRESS/STRAIN: STRONG FORM
4. FINITE ELEMENT APPROXIMATION
5. PROPOSED ELEMENTS
6. NUMERICAL EXAMPLES
7. CONCLUDING REMARKS

A UNIFIED APPROACH TO MIXED FINITE ELEMENT METHODS: APPLICATION TO IN-PLANE PROBLEMS

Shmuel L. Weissman & Robert L. Taylor

Department of Civil Engineering
University of California at Berkeley

1. INTRODUCTION

1.1 Motivation and objective

Over the last two decades much research has been devoted to the design of plane strain elements that do not lock at the nearly incompressible limit. Numerous methods have been proposed (see below). Unfortunately, most of these methods are either based on parameter tuning or cannot be applied to other problems involving internal constraints (e.g., plate bending).

In this work the method presented by Weissman & Taylor [1990] is applied to generate assumed stress and strain fields for four-node plane stress/strain elements. In particular, emphasis is put on proving that the proposed elements do not lock at the nearly incompressible limit. In totality, the proposed elements should exhibit the following properties:

- Resolve locking at the nearly incompressible limit (plain strain) at the element level.
- Recover stresses that are variationally consistent with the formulation used to obtain the displacement field.
- Produce reliable stresses at the element level (without recourse to smoothing).
- Possess correct rank (no spurious energy modes).
- Have performance independent of coordinate system or user input data.

1.2 Background

Solution of plane strain problems at the nearly incompressible limit have traditionally posed severe problems in the development of finite element models. This setback is the result of the failure of finite element models to impose the incompressibility constraint pointwise (e.g., Hughes [1987]).

Much effort has been directed at producing finite element models that avoid the locking phenomenon at the nearly incompressible limit. Initial approaches utilized reduced

integration. However, this approach often results in unstable elements due to the appearance of spurious zero energy modes (Bicanic & Hinton [1979]). To overcome this difficulty, Hughes [1977] used Selective Reduced Integration (SRI). Malkus & Hughes [1978] showed the SRI scheme to fall within the concept of mixed finite element methods. Hughes [1980] refined the SRI scheme into a general method, known as the B-bar method. Simo *et al.* [1985] showed that the B-bar method can be derived from the Hu-Washizu variational principle.

Using a projection operator, Flanagan & Belytschko [1981] showed that the usual finite element approximation can be rewritten in a form that leads to decoupling of the stiffness matrix, which can be written as the sum of the decoupled under-integrated stiffness matrix and a "stabilization" stiffness matrix. Following this approach Belytschko & Bachrach [1986] presented formulations based upon the Hu-Washizu functional. The best of the elements presented is known as the Quintessential Bending Incompressible (QBI). This element, however, is not frame invariant (i.e., it is dependent upon the coordinate system) unless a unique local coordinate system is defined and the element stiffness matrix and load vector, defined in the local coordinate system, are transformed to the global coordinate system.

Wilson, *et al.* [1973] took yet another approach. They observed that when the four-node element (isoparametric displacement formulation) is subjected to pure bending it deforms in shear rather than in bending. As a result of this anomaly, the element is stiff in bending. In order to improve the element bending behavior, they introduced a set of incompatible displacements. It was soon realized, however, that the distorted element did not pass the constant strain patch test. Taylor, *et al.* [1976] modified the incompatible modes element so that the resulting element passed the patch test. In addition to the improved behavior in bending this element avoids locking at the nearly incompressible limit (this property was not observed, however, when the elements were first presented). Conditions for convergence when incompatible modes are used were presented by Strang & Fix [1973].

Pian & Sumihara [1984] used incompatible displacements to generate an assumed stress field for a four-node plane stress element, which was formulated via the Hellinger-Reissner variational principle. This element exhibits excellent characteristics in bending applications. In addition, its sensitivity to mesh distortion from a parallelogram shape appears to be among the smallest of four-node elements. Furthermore, when modified to account for plane strain constitutive relations, it avoids locking at the nearly incompressible limit. Initially, the formulation required a quadratic perturbation of the element shape. Recently, Pian & Wu [1988] presented a new formulation that avoids this perturbation. A

general formulation to generate incompatible element functions was presented by Wu, *et al.* [1987].

Simo & Rifai [1989] presented four-node elements based upon the Hu-Washizu functional which introduced "enhanced strains." Results reported for these elements are almost identical to the results obtained by the element presented by Pian & Sumihara [1984].

Weissman & Taylor [1990] proposed a general method to generate assumed stress and strain field in the context of mixed finite element methods. In order to avoid the limitation principle as put forth by Fraeijs de Veubeke [1965], the assumed fields must satisfy the equilibrium equations at least in a weak sense. Consequently, the assumed fields are constructed to satisfy the homogeneous equilibrium equations in a weak sense. As a result, the internal constraints are satisfied *a priori*.

1.3 Paper overview

The stress and strain field generation procedure is reviewed in Section 2. The strong form for the plane stress and plane strain problems is summarized in Section 3. The finite element approximation is contained in Section 4.

In Section 5 four-node quadrilateral elements formulated via either the Hellinger-Reissner or the Hu-Washizu functionals are proposed for both the plane stress and plane strain problems. It is proved that in the case of plane strain the trace of the assumed strain vanishes, pointwise, as the nearly incompressible limit is approached. Consequently, locking is avoided.

Numerical examples demonstrating the excellent properties of the proposed elements are presented in Section 6. Concluding remarks are given in Section 7.

2. SUMMARY OF ASSUMED FIELDS GENERATION PROCEDURE

Internal constraints pose a difficult problem for finite element methods, commonly manifested by locking. This difficulty was put in the form of a limitation principle by Fraeijs de Veubeke [1965]. In order to avoid this limitation principle, the assumed stress and strain fields must satisfy *a priori* the equilibrium equations and thus, effectively satisfy the internal constraints. In the context of finite element methods this requirement can be relaxed, and the equilibrium equations can be satisfied in a weak sense.

Taking advantage of this observation, Weissman & Taylor [1990] presented a general method to generate assumed stress and strain fields. These fields are constructed to satisfy in a weak sense the homogeneous equilibrium equations and consequently, the internal

constraints. This method is formulated within the framework provided by the Hu-Washizu variational principle, and is summarized below.

Before proceeding to describe the proposed method it is useful to recall the steps involved in deriving finite elements via the Hu-Washizu functional. To this end let ϵ, σ, and $\mathbf{U}$ denote the assumed strain, stress and displacement fields, respectively; $\mathbf{L}$ the strain displacement operator; and $\mathbf{D}$ the elastic coefficients matrix. The Hu-Washizu functional, for the case of small deformations and linear elastic materials (ignoring initial stresses and strains) is given by:

$$\Pi_H(\sigma,\epsilon,\mathbf{U}) := \int_\Omega \left[\frac{1}{2}\epsilon^T \mathbf{D}\epsilon + \sigma^T(\mathbf{L}\mathbf{U}-\epsilon) \right] d\Omega - \Pi_{EXT}(\mathbf{U}) \tag{2.1}$$

where Ω is the domain, and Π_{EXT} is the external work.

The weak, or variational, form may be obtained from the energy functional, Π_H, by making is stationary. This result is obtained by taking the first total variation of Π_H and equating it to zero. To this end, let $\delta\epsilon$, $\delta\sigma$, and $\delta\mathbf{U}$ denote virtual strain, stress and displacement fields, respectively. The weak form is given by:

$$D\Pi_H := \int_\Omega \left[\delta\epsilon^T(\mathbf{D}\epsilon-\sigma) + \delta\sigma^T(\mathbf{L}\mathbf{U}-\epsilon) + (\mathbf{L}\delta\mathbf{U})^T\sigma - \delta\mathbf{U}^T\mathbf{b} \right] d\Omega$$
$$- \int_{Ct} \delta\mathbf{U}^T\sigma^a \, d\Gamma = 0 \tag{2.2}$$

where $\mathbf{b}$ is the body force vector, σ^a are applied traction boundary conditions, and Ct is the part of the boundary on which traction boundary conditions are specified.

The finite element model is obtained by approximating the assumed fields. To this end, let the assumed fields be approximated over each element domain by:

- Stress field: $\sigma = \mathbf{S}\,\mathbf{s}$
- Strain field: $\epsilon = \mathbf{E}\,\mathbf{e}$
- Displacement field: $\mathbf{U} = \mathbf{N}\,\mathbf{d}$

where $\mathbf{S}$, $\mathbf{E}$, and $\mathbf{N}$ are the shape functions for the approximating stress, strain and displacement fields, respectively; and $\mathbf{s}$, $\mathbf{e}$, and $\mathbf{d}$ are the vectors of independent stress, strain, and displacement parameters, respectively.

Substituting the assumed fields into the weak form leads to the following system of equations (these are the approximated Euler-Lagrange equations):

$$\begin{bmatrix} \mathbf{H} & -\mathbf{A}^T & \mathbf{0} \\ -\mathbf{A} & \mathbf{0} & \mathbf{G} \\ \mathbf{0} & \mathbf{G}^T & \mathbf{0} \end{bmatrix} \begin{bmatrix} \mathbf{e} \\ \mathbf{s} \\ \mathbf{d} \end{bmatrix} = \begin{bmatrix} \mathbf{0} \\ \mathbf{0} \\ \mathbf{f} \end{bmatrix} \tag{2.3}$$

where

$$\mathbf{H} := \int_\Omega \mathbf{E}^T \mathbf{D} \mathbf{E} \, d\Omega \quad ; \quad \mathbf{A} := \int_\Omega \mathbf{S}^T \mathbf{E} \, d\Omega \tag{2.4a}$$

$$\mathbf{G} := \int_\Omega \mathbf{S}^T \mathbf{B} \, d\Omega \quad ; \quad \mathbf{f} := \int_\Omega \mathbf{N}^T \mathbf{b} \, d\Omega + \int_{C_t} \mathbf{N}^T \sigma^a \, d\Gamma \tag{2.4b}$$

and $\mathbf{B}$ is defined by: $\mathbf{B} := \mathbf{L}\mathbf{N}$.

Eliminating the stress and strain coefficients, yields:

$$\mathbf{K}\mathbf{d} = \mathbf{f} \tag{2.5}$$

where $\mathbf{K}$ is the element stiffness matrix, given by:

$$\mathbf{K} = \mathbf{G}^T (\mathbf{A}\mathbf{H}^{-1}\mathbf{A}^T)^{-1}\mathbf{G} \tag{2.6}$$

To satisfy stability conditions for every admissible displacement, the following inequalities must hold (Zienkiewicz, *et al.* [1986]):

$$n_e + n_d \geq n_s \quad ; \quad n_s \geq n_d \tag{2.7}$$

where n_e, n_s, and n_d are the number of strain, stress, and displacement parameters, respectively (n_d is equal to the number of nodal degrees-of-freedom).

It is worthwhile noticing that a significant reduction in the computational effort can be obtained if $\mathbf{A}$ is invertible. Henceforth, $\mathbf{A}$ is assumed to be invertible. As a result, $n_e = n_s$ and consequently, the mixed patch test (Zienkiewicz, *et al.* [1986]) provides the minimal number of independent stress and strain parameters. Furthermore, in view of the desire to minimize computations, this is the optimal number.

As was stated above, the underling idea behind the proposed method is to construct assumed stress and strain fields so that they satisfy the homogeneous equilibrium equations in a weak sense. To this end, let the assumed strain field be given as the sum of two independent fields as follows:

$$\epsilon := \bar{\epsilon}^c + \epsilon^i \tag{2.8}$$

and let, for convenience, ϵ^i be given by:

$$\epsilon^i := \mathbf{L}\mathbf{U}^i \tag{2.9}$$

where $\mathbf{U}^i$ is a displacement field not contained in $\mathbf{U}^h$, which is the finite element approximation of the admissible displacement solution space.

The initially assumed stress, $\bar{\sigma}$, and compatible strain, $\bar{\epsilon}^c$, fields are constrained so that the contribution to the energy functional, Π_H, from the mixed terms containing ϵ^I and either $\bar{\epsilon}^c$ or $\bar{\sigma}$ vanishes in a weak sense over each element's domain. As a result, the reduced stress, σ, and compatible strain, ϵ^c, satisfy the homogeneous equilibrium

equations in a weak sense. Furthermore, it follows from the variational structure that the incompatible strain, ϵ^i, is zero pointwise (at the solution). The proposed method is summarized in Box 2.1.

Box 2.1: Proposed Method

1. Select initial assumed (enriched) strain field, $\bar{\epsilon}^c$, and stress field, $\bar{\sigma}$ (Pascal triangle).
2. Select the incompatible strain field, ϵ^i, ($\mathbf{U}^i \notin \mathbf{U}^h$).
3. Reduce the number of independent variables in $\bar{\epsilon}^c$ and $\bar{\sigma}$ by introducing the following constraints:

$$\int_\Omega \mathbf{U}^i_{,i}\, d\Omega = 0$$

$$\int_\Omega \epsilon^{iT} \bar{\sigma}\, d\Omega = \mathbf{0} \qquad \rightarrow \sigma$$

$$\int_\Omega \epsilon^{iT} \bar{\mathbf{D}} \bar{\epsilon}^c\, d\Omega = \mathbf{0} \qquad \rightarrow \epsilon^c$$

4. Substitute the reduced fields into the variational principle.

where $\bar{\mathbf{D}}$ is the mean value of $\mathbf{D}$, defined by: $\bar{\mathbf{D}} := \int_\Omega \mathbf{D}\, d\Omega / \int_\Omega d\Omega$.

$\bar{\mathbf{D}}$ and the constraint equation on $\mathbf{U}^i$ are introduced in order to maintain the constant terms in the initial fields $\bar{\sigma}$ and $\bar{\epsilon}^c$ decoupled from the non-constant terms also in the reduced fields (i.e., conserve the ability to pass the constant stress/strain patch test). The condition $\mathbf{U}^i \notin \mathbf{U}^h$ (in step 2) is introduced in order to prevent the appearance of spurious zero energy modes.

Remark: Recall that the Hellinger-Reissner functional can be obtained from the Hu-Washizu functional by enforcing the stress strain relationship (i.e., $\sigma = \mathbf{D}\epsilon$) pointwise. If this relationship is substituted directly into the Hu-Washizu functional ϵ^i drops out and consequently, the proposed method cannot be used. However, if the formulation is started with a Hu-Washizu functional and the constraints enforced there, while taking notice of the special choice for the strain field, then the same reduced stress field is obtained and ϵ^i drops out only after obtaining the desired stress field.

3. STRONG FORM

The strong, or classical, form for both the plane stress and plane strain problems is presented. Throughout this section Greek subscripts take the values 1 and 2. Repeated indices imply the usual summation convention. All quantities are referred to a fixed system of rectangular, Cartesian coordinates. A general point in this system is denoted by (x_1, x_2, x_3).

The domain of interest is a three-dimensional body embedded in an Euclidian three-space $\mathbf{R}^3$. In the undeformed configuration the domain Ω is of the following form:

$$\Omega := \left\{ (x_1, x_2, x_3) \in \mathbf{R}^3 \mid x_3 \in [\frac{-h(x_1,x_2)}{2}, \frac{+h(x_1,x_2)}{2}], (x_1, x_2) \in A \subset \mathbf{R}^2 \right\}$$

where h is the thickness in the x_3 direction* and A is a closed region bounded by a simple closed curve C with an outgoing unit normal ν. Let C_U and C_t be subregions of C such that $\overline{C_U \bigcup C_t} = C$ and $C_U \bigcap C_t = \phi$, where C_U is the part of C on which displacements are specified and C_t is the part of C on which tractions are specified.

The strong form is summarized in Box 3.1

Box 3.1: Plane stress/strain - Strong Form

Given b_α, σ^a_α, and U^a_α; find U_α and $\sigma_{\alpha\beta}$ such that:

$$\text{in } A \begin{cases} \sigma_{\alpha\beta,\beta} + b_\alpha = 0 \\ \sigma_{\alpha\beta} = C_{\alpha\beta\gamma\delta}\epsilon_{\gamma\delta} \\ \epsilon_{\alpha\beta} = \frac{1}{2}(U_{\alpha,\beta} + U_{\beta,\alpha}) \end{cases}$$

$$\text{on } C_U \begin{cases} U_\alpha = U^a_\alpha \end{cases}$$

$$\text{on } C_t \begin{cases} \nu_\beta \sigma_{\alpha\beta} = \sigma^a_\alpha \end{cases}$$

* In the case of plane strain $h \equiv 1$.

where b_α are the body forces, σ_α^a are the specified traction boundary conditions, U_α^a are the specified displacement boundary conditions and $C_{\alpha\beta\gamma\delta}$ is the elastic coefficients tensor, which for the case of plane strain is given by:

$$C_{\alpha\beta\gamma\delta} := h\,[\mu\,(\delta_{\alpha\gamma}\delta_{\beta\delta} + \delta_{\alpha\delta}\delta_{\beta\gamma}) + \lambda\,\delta_{\alpha\beta}\delta_{\gamma\delta}] \tag{3.1}$$

where λ and μ are the Lamé coefficients, which can be eliminated in favor of Young's modulus, E, and Poisson's ratio, ν, using

$$\lambda = \frac{\nu E}{(1+\nu)(1-2\nu)} \quad ; \quad \mu = \frac{E}{2(1+\nu)} \tag{3.2}$$

The plane stress elastic coefficients are obtained by replacing λ by $\bar{\lambda}$, where $\bar{\lambda}$ is given by:

$$\bar{\lambda} = \frac{2\mu\lambda}{\lambda + 2\mu} = \frac{\nu E}{1-\nu^2} \tag{3.3}$$

Note that in the case of plane stress, the strain terms in the x_3 direction can be obtained from the constitutive equations. Similarly, in the case of plane strain, the stress terms in the x_3 directions also can be obtained from the constitutive equations. Consequently, the in-plane stress and strain fields characterize the three-dimensional state for both problems.

It follows from Box 3.1 that the strain displacement operator **L** is given by:

$$\mathbf{L} := \begin{bmatrix} \frac{\partial}{\partial x_1} & 0 \\ 0 & \frac{\partial}{\partial x_2} \\ \frac{\partial}{\partial x_2} & \frac{\partial}{\partial x_1} \end{bmatrix} \tag{3.4}$$

and the elastic coefficient matrix, **D**, is given by:

$$\mathbf{D} = \frac{E\,h}{1-\nu^2} \begin{bmatrix} 1 & \nu & 0 \\ \nu & 1 & 0 \\ 0 & 0 & \frac{1}{2}(1-\nu) \end{bmatrix} \tag{3.5a}$$

for the case of plane stress, and by:

$$\mathbf{D} = \frac{E}{(1+\nu)(1-2\nu)} \begin{bmatrix} 1-\nu & \nu & 0 \\ \nu & 1-\nu & 0 \\ 0 & 0 & \frac{1}{2}(1-2\nu) \end{bmatrix} \tag{4.5b}$$

for the case of plane strain.

4 FINITE ELEMENT APPROXIMATION

The method summarized in Section 2 is used to formulate four-node quadrilateral plane stress and plane strain elements. The initially assumed stress and strain fields as well as the incompatible displacements used to generate the assumed incompatible strains are presented. In Section 4.1, the assumed displacement field is introduced. The assumed stress field is given in Section 4.2, and the assumed compatible strains in Section 4.3. The incompatible displacements used to generate the assumed incompatible strains are summarized in Section 4.4.

4.1 Assumed displacement field

The assumed displacement field is taken as a standard isoparametric field. The displacements are approximated by:

$$\mathbf{U} = N_I \, d_I \tag{4.1}$$

where N_I is the shape function associated with node I, and d_I is the nodal displacement vector. In the case of four-node quadrilateral elements, the shape functions are given by:

$$N_I(\xi,\eta) = \frac{1}{4}(1+\xi_I\xi)(1+\eta_I\eta) \tag{4.2}$$

where ξ and η are the element natural coordinates, on the interval [-1,1], and ξ_I and η_I are the values of the natural coordinates at node I.

4.2 Assumed stress fields

The assumed in-plane stress field is a complete linear field* expressed in the element natural coordinates as:

$$\bar{\sigma}^* = \begin{bmatrix} \bar{\sigma}^*_{\xi\xi} \\ \bar{\sigma}^*_{\eta\eta} \\ \bar{\sigma}^*_{\xi\eta} \end{bmatrix} = \begin{bmatrix} 1 & \xi & \eta & 0 & 0 & 0 & 0 & 0 & 0 \\ 0 & 0 & 0 & 1 & \xi & \eta & 0 & 0 & 0 \\ 0 & 0 & 0 & 0 & 0 & 0 & 1 & \xi & \eta \end{bmatrix} \begin{bmatrix} s^*_1 \\ s^*_2 \\ \cdot \\ \cdot \\ s^*_9 \end{bmatrix} \tag{4.3}$$

Since complete polynomials are used to express the in-plane stresses, equation (4.3) could be used for $\bar{\sigma}$ directly. However, the reduction to satisfy the constraints introduced in Box 2.1 would require selection of different parameters in each element (i.e., there would be a dependence on element orientation of ξ and η with respect to x_1 and x_2). This dependence may be avoided by using the transformation procedure described below.

* The stress resultant and strain fields are assumed as complete linear fields since this is the best assumption that may be used in conjunction with a bilinear displacement field.

The following definitions are introduced:

$$xs = \frac{1}{4}\xi_I x_{1I} \;\; ; \;\; xt = \frac{1}{4}\eta_I x_{1I} \;\; ; \;\; xh = \frac{1}{4}(\xi\eta)_I x_{1I}$$

$$ys = \frac{1}{4}\xi_I x_{2I} \;\; ; \;\; yt = \frac{1}{4}\eta_I x_{2I} \;\; ; \;\; yh = \frac{1}{4}(\xi\eta)_I x_{2I}$$

Following Zienkiewicz & Taylor [1989], the Jacobian of the coordinate transformation from the (ξ, η) space to the (x_1, x_2) space is given by:

$$J = J_0 + J_1\xi + J_2\eta \tag{4.4}$$

where,

$$J_0 = xs \cdot yt - xt \cdot ys \tag{4.5a}$$

$$J_1 = xs \cdot yh - xh \cdot ys \tag{4.5b}$$

$$J_2 = xh \cdot yt - xt \cdot yh \tag{4.5c}$$

The stress field in the physical space is obtained by using the following transformation:

$$\sigma_{ij} = \frac{1}{J} F_{iI} F_{kK} \sigma^*_{IK} \tag{4.6}$$

where both i and j take the values x_1 or x_2, and both I and J take the values ξ or η, and $F_{x_i\xi} = \dfrac{\partial x_1}{\partial \xi}$, etc. However, to maintain the ability to model constant fields (i.e., pass the constant strain patch test), the transformation is performed based on the Jacobian, J, and "deformation gradient", F, at the center of the element.

At the center of the element, F is given by:

$$F_{x_1\xi} = xs \;\; ; \;\; F_{x_1\eta} = xt \tag{4.7a}$$

$$F_{x_2\xi} = ys \;\; ; \;\; F_{x_2\eta} = yt \tag{4.7b}$$

After redefining the independent coefficients, the assumed stress field is given by:

$$\bar{\sigma} = \begin{bmatrix} \bar{\sigma}_{11} \\ \bar{\sigma}_{22} \\ \bar{\sigma}_{12} \end{bmatrix} = \begin{bmatrix} 1 & 0 & 0 & xs^2\eta & xt^2\xi & xs^2\xi & xt^2\eta & 2\,xs\,xt\,\xi & 2\,xs\,xt\,\eta \\ 0 & 1 & 0 & ys^2\eta & yt^2\xi & ys^2\xi & yt^2\eta & 2\,ys\,yt\,\xi & 2\,ys\,yt\,\eta \\ 0 & 0 & 1 & xs\,ys\,\eta & xt\,yt\,\xi & xs\,ys\,\xi & xt\,yt\,\eta & A\,\xi & A\,\eta \end{bmatrix} \begin{bmatrix} s_1 \\ s_2 \\ \cdot \\ \cdot \\ s_9 \end{bmatrix} \tag{4.8}$$

where,

$$A = xs \cdot yt + xt \cdot ys$$

$$s_1 = \frac{1}{J_0}(xs^2 s_1^* + xt^2 s_4^* + 2\,xs\,xt\,s_7^*)$$

$$s_2 = \frac{1}{J_0}(ys^2 s_1^* + yt^2 s_4^* + 2\,ys\;yt\;s_7^*)$$

$$s_3 = \frac{1}{J_0}(xs\;ys\;s_1^* + xt\;yt\;s_4^* + A\;s_7^*)$$

$$s_i = \frac{1}{J_0} s_j^*$$

with

$$(i\,,j) \in \Big\{(4,3),(5,5),(6,2),(7,6),(,8,8),(9,9)\Big\}$$

It is convenient to write σ in the following form:

$$\tilde{\sigma} = \left[\hat{\sigma}_1 \mid \hat{\sigma}_2\right] \begin{bmatrix} \hat{s}_1 \\ \hat{s}_2 \end{bmatrix}$$

where,

$$\hat{s}_1^T = < s_1, s_2, s_3, s_4, s_5 > \;;\; \hat{s}_2^T = < s_6, s_7, s_8, s_9 >$$

With the above construction, the parameter set $\hat{s}_2$ may always be selected as the set to be eliminated in satisfying the constraint equation on the stress field (see Box 2.1).

4.3 Assumed strain fields

The assumed strain field is formulated in the element natural coordinates, and then transformed into the physical domain. Two types of transformations can be used:

- The same transformation as used for the corresponding stress fields.
- The inverse to the transformation used for the corresponding stress fields.

The motivation for the first approach is to have the same "shape functions," or interpolation, for the strain fields as for the corresponding stress fields. The second approach is motivated by the invariance of the complementary energy ($\sigma_{ij}\,\epsilon_{ij}$) under coordinate transformation. Accordingly, the transformation is given by*:

$$\epsilon_{ij} = J\,F_{Ii}^{-1} F_{Jj}^{-1} \epsilon_{IJ}^* \tag{4.9}$$

A similar approach was taken by Simo & Rifai [1989].

Following the path established for the assumed stress field, the strain field is assumed as a complete linear field in the element natural coordinates, and then transformed into the physical space. Using the transformation given by equation (4.6) yields:

* The transformation is based on the values at the center of the element.

$$\bar{\epsilon}^c = \begin{bmatrix} \bar{\epsilon}^c_{11} \\ \bar{\epsilon}^c_{22} \\ \bar{\epsilon}^c_{12} \end{bmatrix} = \begin{bmatrix} 1 & 0 & 0 & xs^2\eta & xt^2\xi & xs^2\xi & xt^2\eta & 2xs\,xt\,\xi & 2xs\,xt\,\eta \\ 0 & 1 & 0 & ys^2\eta & yt^2\xi & ys^2\xi & yt^2\eta & 2ys\,yt\,\xi & 2ys\,yt\,\eta \\ 0 & 0 & 1 & xs\,ys\,\eta & xt\,yt\,\xi & xs\,ys\,\xi & xt\,yt\,\eta & A\,\xi & A\,\eta \end{bmatrix} \begin{bmatrix} e_1 \\ e_2 \\ \cdot \\ \cdot \\ e_9 \end{bmatrix} \tag{4.10a}$$

and using the inverse transformation, equation (4.9), yields:

$$\bar{\epsilon}^c = \begin{bmatrix} 1 & 0 & 0 & yt^2\eta & xt^2\xi & yt^2\xi & xt^2\eta & -2yt\,xt\,\xi & -2yt\,xt\,\eta \\ 0 & 1 & 0 & ys^2\eta & xs^2\xi & ys^2\xi & xs^2\eta & -2ys\,xs\,\xi & -2ys\,xs\,\eta \\ 0 & 0 & 1 & -yt\,ys\,\eta & -xt\,xs\,\xi & -yt\,ys\,\xi & -xt\,xs\,\eta & A\,\xi & A\,\eta \end{bmatrix} \begin{bmatrix} e_1 \\ e_2 \\ \cdot \\ \cdot \\ e_9 \end{bmatrix} \tag{4.10b}$$

It is convenient to write ϵ in the following form:

$$\epsilon = \left[\hat{\epsilon}_1 \mid \hat{\epsilon}_2\right] \begin{bmatrix} \hat{e}_1 \\ \hat{e}_2 \end{bmatrix}$$

where,

$$\hat{e}_1^T = < e_1, e_2, e_3, e_4, e_5 > \; ; \; \hat{e}_2^T = < e_6, e_7, e_8, e_9 >$$

With the above construction, the parameter set $\hat{e}_2$ may always be selected as the set to be eliminated in satisfying the constraint equation on the strain field (see Box 2.1).

4.4 Assumed incompatible displacements

Let the assumed incompatible displacements be given by:

$$U_1^i = N_1^i \lambda_1 + N_2^i \lambda_2 \tag{4.11a}$$

and

$$U_2^i = N_1^i \lambda_3 + N_2^i \lambda_4 \tag{4.11b}$$

where λ_1, λ_2, ..., and λ_4 are the independent incompatible displacement parameters, and N_α^i are the incompatible shape functions.

Two options are selected for the incompatible shape functions N_1^i and N_2^i. The first set was presented by Wu, *et al.* [1987]. The functions are given by:

$$N_1^i = \xi^2 - \frac{2J_1}{3J_0}\xi + \frac{2J_2}{3J_0}\eta \tag{4.12a}$$

and

$$N_2^i = \eta^2 + \frac{2J_1}{3J_0}\xi - \frac{2J_2}{3J_0}\eta \tag{4.12b}$$

The second set was presented by Taylor, *et al.* [1986]. In order to obtain a more compact form, the incompatible modes given below are a linear combination of the modes originally presented. The functions are given by:

$$N_1^i = (1 - \frac{J_2}{J_0}\eta)(1-\xi^2) + \frac{J_1}{J_0}\xi(1-\eta^2) \tag{4.13a}$$

and

$$N_2^i = (1 - \frac{J_1}{J_0}\xi)(1-\eta^2) + \frac{J_2}{J_0}\eta(1-\xi^2) \tag{4.13b}$$

Note that the second set of incompatible modes is zero (compatible) at the nodal points while the first set is not.

5. PROPOSED ELEMENTS

The fields presented in Section 4 are used to generate four-node plane stress/strain elements. The proposed elements are cataloged in Table 5.1 by the type of formulation, the incompatible shape functions, and assumed strain field (Hu-Washizu). For all these elements, the assumed displacement and stress fields are given by equations (4.1) and (4.8), respectively.

Table 5.1 Proposed Plane Stress/Strain Elements

Element	Formulation	Incompatible shape function equations	Strain field representation
PSS1	Hellinger-Reissner	(4.12)	-
PSS2	Hellinger-Reissner	(4.13)	-
PSS3	Hu-Washizu	(4.12)	(4.10a)
PSS4	Hu-Washizu	(4.13)	(4.10a)
PSS5	Hu-Washizu	(4.12)	(4.10b)
PSS6	Hu-Washizu	(4.13)	(4.10b)

The remainder of this section consists of proofs (for the case of plane strain) showing that as the incompressible limit is approached, the assumed strain vanishes pointwise for the proposed elements. Consequently, the well-known locking behavior is avoided at the element level. The proof for elements formulated via the Hellinger-Reissner and Hu-Washizu variational principles are given in Propositions 5.1 and 5.2, respectively.

Proposition 5.1: The Hellinger-Reissner elements presented above can, in the case of plane strain, model a state in which the trace of the strain goes to zero, pointwise, as ν goes to 0.5^-.

Proof: Recall that in the case of the Hellinger-Reissner variational principle the assumed strain field is obtained from the assumed independent stress field. Consequently, in the case of plane strain the strain field ϵ is given by:

$$\epsilon = \mathbf{D}^{-1}\sigma \tag{5.1}$$

where $\mathbf{D}^{-1}$ is given by:

$$\mathbf{D}^{-1} = \frac{1}{\alpha}\begin{bmatrix} \lambda+2\mu & -\lambda & 0 \\ -\lambda & \lambda+2\mu & 0 \\ 0 & 0 & \frac{\alpha}{\mu} \end{bmatrix} \tag{5.2}$$

with,

$$\alpha = 4\mu(\mu+\lambda)$$

As Poisson's ratio, ν, goes to 0.5^{-}, λ goes to infinity while μ remains bounded. It follows that, at the limit, the following relation is obtained:

$$\mathbf{D}_{11}^{-1} = \mathbf{D}_{22}^{-1} = -\mathbf{D}_{12}^{-1} = -\mathbf{D}_{21}^{-1} \tag{5.3}$$

After imposing the constraint equations introduced in Section 3, the assumed stress field presented in equation (4.8) is reduced to the general form:

$$\sigma = \begin{bmatrix}\sigma_{11}\\ \sigma_{22}\\ \sigma_{12}\end{bmatrix} = \begin{bmatrix} 1 & 0 & 0 & a_1\eta + b_1\xi & a_4\xi + b_4\eta \\ 0 & 1 & 0 & a_2\eta + b_2\xi & a_5\xi + b_5\eta \\ 0 & 0 & 1 & a_3\eta + b_3\xi & a_6\xi + b_6\eta \end{bmatrix} \begin{bmatrix} s_1 \\ s_2 \\ \cdot \\ \cdot \\ s_5 \end{bmatrix} \tag{5.4}$$

where a_1, a_2, ..., and a_6, and b_1, b_2, ..., and b_6 are constants to be determined by the procedure presented in Box 2.1.

Substituting equations (5.2) and (5.4) into equation (5.1) and taking notice of equation (5.3) yields the desired result. ▪

Proposition 5.2: The Hu-Washizu elements presented above can, in the case of plane strain, model a state in which the trace of the strain field goes to zero, pointwise, as the incompressible limit is approached.

Proof: After constraining the assumed strain field introduced in equations (4.10), the reduced field is given in a general form by:

$$\epsilon = \begin{bmatrix} \epsilon_{11} \\ \epsilon_{22} \\ \epsilon_{12} \end{bmatrix} = \begin{bmatrix} 1 & 0 & 0 & a_1\eta + b_1\xi & a_4\xi + b_4\eta \\ 0 & 1 & 0 & a_2\eta + b_2\xi & a_5\xi + b_5\eta \\ 0 & 0 & 1 & a_3\eta + b_3\xi & a_6\xi + b_6\eta \end{bmatrix} \begin{bmatrix} p_1 \\ p_2 \\ \cdot \\ \cdot \\ p_5 \end{bmatrix} \tag{5.5}$$

The structure imposed by the constraint equations is such that the following relations are obtained, as ν goes to 0.5^-, between the a_1, a_2, ..., and a_6 and b_1, b_2, ..., b_6 coefficients:

$$a_1 + a_2 = 0 \quad ; \quad a_4 + a_5 = 0 \tag{5.6a}$$

and

$$b_1 + b_2 = 0 \quad ; \quad b_4 + b_5 = 0 \tag{5.6b}$$

A formal proof for equations (5.6) can be obtained. This proof, however, is very cumbersome and tedious, and does not yield a better understanding of the formulation. For these reasons, a numerical "proof" will be given. To obtain a more compact form, an equivalent form to equations (5.6) is given. Namely, the values of $(a_1 + a_2)\eta + (b_1 + b_2)\xi$ and $(a_4 + a_5)\xi + (b_4 + b_5)\eta$ are reported at the Gauss points. Since the functions are linear, zero value at all Gauss points implies zero value pointwise. First, a square element (see Figure 5.1a) is examined. The values for the first Gauss point are reported in Table 5.2. Values for other Gauss points may be obtained as follows: given that the value at the first point is v, then at the other points it is - sign(ξ) * v, where sign(ξ) is the sign of the ξ or η coordinate at the given Gauss point (η for the first column and ξ for the second column).

Table 5.2 Square element

ν	$(a_1 + a_2)\eta + (b_1 + b_2)\xi$	$(a_4 + a_5)\xi + (b_4 + b_5)\eta$
0.	-0.144338	-0.144338
0.3	-0.082479	-0.082479
0.49	-0.005661	-0.005661
0.499	-0.000577	-0.000577
0.4999	-0.000058	-0.000058

Secondly, an element distorted from a parallelogram shape (see Figure 5.1b) is examined. In this case the values at the first and second Gauss points are reported. The value for the third Gauss point is minus the value at the second Gauss point, and the value at the forth Gauss point is minus the value at the second Gauss point. Results are summarized in Tables 5.3 and 5.4. The results summarized in Tables 5.1, 5.2 and 5.3 "prove" equations (5.6).

Table 5.3 Distorted element					
ν	point	$(a_1+a_2)\eta+(b_1+b_2)\xi$			
		PSS3	PSS4	PSS5	PSS6
0.	1	-0.138299	-0.136318	-0.239751	-0.166003
	2	-0.142666	-0.145547	-0.234665	-0.224427
0.3	1	-0.074126	-0.072729	-0.2255061	-0.231639
	2	-0.077283	-0.079388	-0.204323	-0.169421
0.49	1	-0.004723	-0.004612	-0.051700	-0.037454
	2	-0.004982	-0.005156	-0.055967	-0.042924
0.499	1	-0.000479	-0.000467	-0.006410	-0.004384
	2	-0.000505	-0.000523	-0.006890	-0.004980
0.4999	1	-0.000048	-0.000047	-0.000650	-0.000446
	2	-0.000051	-0.000052	-0.000700	-0.000506

Table 5.4 Distorted element					
ν	point	$(a_4+a_5)\xi+(b_4+b_5)\eta$			
		PSS3	PSS4	PSS5	PSS6
0.	1	-0.099318	-0.096704	-0.386263	-0.414609
	2	+0.102311	+0.103024	+0.388999	+0.420426
0.3	1	-0.053029	-0.051169	-0.692734	-1.013897
	2	+0.055193	+0.055728	+0.703892	+1.045209
0.49	1	-0.003365	-0.003215	+0.027529	+0.021353
	2	+0.003542	+0.003588	-0.029822	-0.024105
0.499	1	-0.000341	-0.000326	+0.002510	+0.001978
	2	+0.000359	+0.000364	-0.002771	-0.002279
0.4999	1	-0.000034	-0.000033	+0.000249	+0.000197
	2	+0.000036	+0.000036	-0.000276	-0.000227

It follows from equations (4.12) and (4.13) that as ν goes to 0.5^- the trace of ϵ is given by:

$$trace(\epsilon) = e_1 + e_2 \tag{5.7}$$

In order to show that the trace of the strain goes to zero pointwise recall from Section 2 that the stress strain weak relation is given by:

$$\mathbf{H}\mathbf{e} - \mathbf{A}\mathbf{s} = 0 \tag{5.8}$$

To simplify notations and without loss of generality, ξ and η in the assumed strain field, equation (5.5), may be replaced by $\bar{\xi}$ and $\bar{\eta}$, given by:

$$\bar{\xi} = \xi - \xi_0 \quad ; \quad \bar{\eta} = \eta - \eta_0$$

where ξ_0 and η_0 are shifts introduced in order to make $\mathbf{H}^n$ block diagonal. In order to

obtain this result the following requirements must be met:

$$\int_A \bar{\xi}\, dA = 0 \quad ; \quad \int_A \bar{\eta}\, dA = 0$$

The resulting ξ_0 and η_0 are given by:

$$\xi_0 = \frac{J_1}{3J_0} \quad ; \quad \eta_0 = \frac{J_2}{3J_0}$$

The **H** matrix is now of the following form:

$$\mathbf{H} = \begin{bmatrix} \mathbf{D}A & 0 \\ 0 & \hat{\mathbf{H}} \end{bmatrix} \tag{5.9}$$

where **D** is given by equation (3.5), A is the element area, and $\hat{\mathbf{H}}$ is the "material" properties for the linear part of the strains field. Based on results in equations (5.6), $\hat{\mathbf{H}}\hat{\mathbf{e}}$ ($\hat{\mathbf{e}}^T = \left\{ e_4, e_5 \right\}$) goes to zero pointwise as the incompressible limit is approached. Hence, it remains only to consider the constant part, given by $\mathbf{D}A$.

Combining equations (5.8) and (5.9) yields:

$$e_1 = \frac{1}{\alpha A} \left\{ (\lambda + 2\mu)\bar{s}_1 - \lambda \bar{s}_2 \right\} \tag{5.10a}$$

and

$$e_2 = \frac{1}{\alpha A} \left\{ (\lambda + 2\mu)\bar{s}_2 - \lambda \bar{s}_1 \right\} \tag{5.10b}$$

where $\bar{\mathbf{s}} = \mathbf{A}\mathbf{s}$.

Substituting equations (5.10) into equation (5.7) yields:

$$trace(\mathbf{e}) = \frac{2\mu(\bar{s}_1 + \bar{s}_2)}{\alpha A} \tag{5.11}$$

As ν goes to 0.5^-, α goes to infinity while μ is bounded; hence the desired result is obtained. ▪

6. NUMERICAL EXAMPLES

The performance of the plane stress/strain (PSS) elements proposed in Section 5 is evaluated with several discriminating problems selected from the literature. The purpose of these evaluations is to test the proposed formulation's sensitivity to the specific choice of the incompatible shape functions as well as the overall performance of the proposed elements.

First tackled are the constant strain patch tests in Section 6.1. Following these are the beam problems suggested by MacNeal & Harder [1985] in Section 6.2, sensitivity to mesh distortion in Section 6.3, the Cook membrane (Cook [1987]) in Section 6.4, the thick walled cylinder also introduced by MacNeal & Harder [1985] in Section 6.5, and a strip of finite width with a hole in Section 6.6.

Convergence of the results obtained by the four-node elements presented in this paper are compared with other well-known four-node plane stress/strain elements. A listing of these elements, and the abbreviations used to identify them is given in Table 4.4.

Table 6.1 Reference Elements

Element	Description
2X2	Isoparametric plane stress/strain.
P-S	Pian & Sumihara [1984], plane stress/strain.
QBI	Belytschko & Bachrach [1986], plane stress/strain.

In all the examples given in this paper, identical results are obtained for elements formulated via the Hellinger-Reissner variational principle and the corresponding (i.e., same incompatible shape functions) elements formulated via the Hu-Washizu variational principle. Identical results are also obtained for the two approaches taken to transform the assumed strain field from the element's natural space into the physical space.

Convergence is examined in the energy norm (energy norm reported is twice the internal strain energy) since this is the natural convergence test in the context of finite element methods (Strang & Fix [1973]). Convergence of displacement at some characteristic points is also examined as this is the common practice in the literature. All tables and figures show the displacement/energy norm as a function of the number of elements (denoted nel) used in the corresponding mesh.

6.1 Patch test

A rectangular domain is modeled by a single element shown in Figure 6.1a and the skewed mesh shown in Figure 6.1b. The mesh is subjected to a constant state of tension/compression. All elements presented pass this test.

6.2 Beam problems: in-plane shear

These problems were suggested by MacNeal & Harder [1985] as standard problems to evaluate the performance of different elements. The meshes used contain only one row of six elements for both the straight beams, shown in Figure 6.2, and the curved beam, shown in Figure 6.3. Geometrical and material properties used are summarized in Table 6.2.

Table 6.2 Material and Geometrical Properties for Beam Problems						
	E	ν	thickness	length/ inner radius	width/ outer radius	arc
straight beam	1.0E+7	0.3	0.1	6.0	0.2	-
curved beam	1.0E+7	0.25	0.1	4.12	4.32	90^o

The "exact" tip displacement, w, given by beam theory (MacNeal & Harder [1985]) for the case of a straight beam is $w = 0.1081$ and for the case of a curved beam is $w = 0.08734$. The results, normalized with respect to the exact solution, are summarized in Table 6.3.

Table 6.3 In-plane shear			
mesh	PSS/P-S	2X2	QBI
straight (a)	0.9929	0.0933	0.9929
straight (b)	0.2208	0.0278	0.0777
straight (c)	0.7963	0.0348	0.0890
curved	0.9782	0.0740	0.2324

Results obtained for all proposed elements are identical to the results obtained by the Pian & Sumihara [1984] element. The 2X2 element locks for all meshes. However, if two rows of elements are used, the 2X2 element yields reasonable results. All elements exhibit locking when trapezoid-shape elements are used (straight mesh (b)). This is in accordance with the theorem put forth by MacNeal [1987] regarding the locking of tapered four-node membrane elements. The QBI element appears to be much more sensitive to mesh distortion than the PSS or P-S elements.

6.3 Beam bending: Sensitivity to mesh distortion

In this standard test, a beam is modeled by two elements. The beam is fixed at one end and subjected to a bending moment on the other, as shown in Figure 6.4. The material properties used are: E = 1.0 and ν = 0.4999. A state of plane strain is assumed. The edge separating the two elements is gradually rotated, as shown in the figure, to skew the mesh. Results, normalized with the exact beam theory solution (w = 562.575), are shown in Figure 6.5. Results for the 2X2 element are not reported since it exhibits severe locking.

All proposed elements yield identical results to the Pian & Sumihara [1984] element. The QBI element exhibits rapid deterioration as Δ is increased.

6.4 Cook's membrane problem

The problem consists of a trapezoidal plate clamped on one end and loaded by a uniformly distributed in-plane bending load on the other end, as shown in Figure 6.6. This problem has a considerable amount of shear deformation. It was suggested by Cook [1987] as an excellent problem to test membrane elements using skewed meshes. No analytical solution is available for this problem. The best known solution is given by Cook as: V_C = 0.29 (vertical displacement), σ_A = 0.236 (maximum principal stress) and σ_B = –0.201 (minimum principal stress). The material properties used are: E = 1.0, ν = 1.0/3.0, thickness = 1.0; plane stress assumption was used. The results normalized with respect to these best known answers are shown in Figures 6.7 (V_C), 6.8 (σ_A) and 6.9 (σ_B).

The results presented for one element are obtained by interpolating the nodal values; for the finer meshes the nodal values are reported. The results obtained for all proposed elements yield identical results to the Pian & Sumihara [1984] element. Excellent results are obtained even for very coarse meshes; about 70% of the vertical displacement and 80% of the stresses are obtained using only one element. The 2X2 and QBI elements yield poor results for coarse meshes; less than 50% and 60% of the vertical displacement and stresses are obtained by the 2X2 and QBI elements, respectively, when a four-element mesh is used.

6.5 Thick-walled cylinder

This problem was suggested by MacNeal & Harder [1985] as an excellent problem to test the effect of nearly incompressible material. The mesh used is shown in Figure 6.10. The material properties are: E = 1.0 and ν varies from 0.0 to 0.4999. The exact radial solution is given by:

$$u = \frac{(1+\nu)p\,R_1^2}{E\,(R_2^2 - R_1^2)}\left[\frac{R_2^2}{r} + (1-2\nu)r\right] \tag{6.1}$$

where p is the internal pressure; R_1 is the inner radius; R_2 is the outer radius; and r is the radius where the radial displacement, u, is to be computed.

Results, normalized with respect to the exact solution, are summarized in Table 6.4.

Once again all proposed plane elements yield identical results with the Pian & Sumihara [1984] element. Almost no deterioration with ν is observed, only 0.77% difference between the two extreme values of ν. The QBI element yields almost identical results. The 2X2 element exhibits the well known locking at the nearly incompressible limit.

Table 6.4 Thick-Walled Cylinder			
ν	PSS/P-S	2X2	QBI
0.	0.9987	0.9964	0.9985
0.3	0.9954	0.9908	0.9952
0.49	0.9913	0.8490	0.9911
0.499	0.9910	0.3606	0.9909
0.4999	0.9910	0.0534	0.9908

6.6 Finite strip with a hole

This problem is introduced in order to test the accuracy of the stress distribution inside the proposed plane elements. A strip of finite width with a hole, of width b, is subjected to uniform tensile stress in the axial direction, as shown in Figure 6.11. The axial stress along the critical section, line A-B, is investigated.

First, the relatively simple case of plane stress with free upper and lower edges is investigated in Section 6.6.1. Then, the more challenging case of plane strain, at the nearly incompressible limit, with the upper and lower edges fixed in the vertical direction, is tackled in Section 6.6.2.

6.6.1 Finite strip with a hole: Plane stress

The material properties used are E = 1.0 and ν = 0.3. First, convergence in the energy norm is examined. No analytical solution for the energy is known. Therefore, a converged finite element solution of 19.37 obtained for the Pian & Sumihara [1984] element using 3072 elements is used as the reference solution. Results normalized with respect to this reference solution are shown in Figure 6.12. The axial stress distribution along the critical section for the meshes containing 48 and 192 elements is presented in Figure 6.13. The results are compared with a reference solution given by Savin [1961].

Almost identical results are obtained for the proposed elements and the Pian & Sumihara element (about 5.0E-3 difference in energy norm for the three-element mesh). A very small sensitivity to the incompatible shape functions used is observed (about 2.0E-3 difference in the energy norm for the three-element mesh).

Excellent results are obtained for both the energy norm, 95.82% of the reference solution with only three elements, and stress distribution inside the elements. The 2X2 and QBI elements yield comparable results for this problem.

6.6.2 Finite strip with a hole: Plane strain

The material properties used are E = 1.0 and ν = 0.4999. First, convergence in the energy norm is examined. No analytical solution for the energy is available. Therefore, a converged finite element solution of 2.389 obtained for the Pian & Sumihara [1984] element using 12288 elements is used as the reference solution. Results normalized with respect to this reference solution are shown in Figure 6.14. The axial stress distribution along the critical section for the meshes containing 48 and 192 elements is presented in Figure 6.15. No analytical solution for the stress distribution is available. Therefore, the smoothed stresses obtained for the 768-element mesh are used as a reference.

The results obtained show the Pian & Sumihara element to exhibit a marginal superiority over the proposed elements for the coarse meshes, only 0.8% for a twelve-element mesh. The formulation shows a small sensitivity to the type of incompatible shape functions used, only 1.3% and 0.04% for three- and twelve-element meshes, respectively.

Excellent results are obtained; with only three elements in the mesh, 69% and 68% of the reference solution is obtained for the PSS1,3,5 and PSS2,4,6, respectively. Excellent results are also obtained for the stress distribution inside the elements.

7. CONCLUDING REMARKS

The main objective of this paper is to apply the method proposed by Weissman & Taylor [1990] to generate assumed fields for four-node quadrilateral plane stress/strain elements. One of the method's main goals is to avoid locking, which is commonly observed in finite element models of problems involving internal constraints. As an illustration of the treatment of internal constraints, the problem of plane strain at the nearly incompressible limit is chosen due to the difficulty it presents to finite element methods, and the large body of work which has been directed toward eliminating this obstacle.

Both elements formulated via the Hellinger-Reissner and Hu-Washizu variational principle are considered. For both types of formulations, it is proven that as the nearly incompressible limit is approached (plane strain), the trace of the strain vanishes pointwise (i.e., the internal constraint is satisfied pointwise). Consequently, locking at the nearly incompressible limit is avoided.

The proposed elements are subjected to an extensive set of problems reported in the literature. Excellent results are obtained for all examples. In fact the results are equivalent to those obtained by the best known elements (e.g., Pian & Sumihara [1984]). Furthermore, the variationally consistent stresses recovered at the element level yield excellent results.

Identical results are obtained for elements formulated via the Hellinger-Reissner and Hu-Washizu functionals, provided the same incompatible functions are used. Also, identical results are obtained for both approaches taken to transform the assumed strain field from the element's natural space into the physical space. Furthermore, results show no sensitivity to the incompatible shape functions used.

REFERENCES

Belytschko, T. & W.E. Bachrach, [1986], "Efficient Implementation of Quadrilaterals With High Coarse-Mesh Accuracy," *Computer Methods in Applied Mechanics and Engineering*, Vol. 54, pp. 279-301.

Bicanic, N. & E. Hinton, [1979], "Spurious Modes in Two-Dimensional Isoparametric Elements," *International Journal for Numerical Methods in Engineering, Vol. 14, pp. 1545-1557.*

Cook, R. D. [1987], "A Plane Hybrid Element With Rotational d.o.f. and Adjustable Stiffness," *International Journal for Numerical Methods in Engineering*, Vol. 24, pp. 1499-1508.

Flanagan, D.P., & T. Belytschko, [1981], "A Uniform Strain Hexahedron and Quadrilateral With Orthogonal Hourglass Control," *International Journal for Numerical Methods in Engineering*, Vol. 17, pp. 679-706.

Fraeijs de Veubeke, B., [1965], "Displacement and Equilibrium Models in the Finite Element Method," in *Stress Analysis*, editors O.C. Zienkiewicz & G.S. Holister. London: John Wiley.

Hughes, T.J.R., [1977], "Equivalence of Finite Elements for Nearly Incompressible Elasticity," *Journal of Applied Mechanics, Vol. 44, pp. 181-183.*

Hughes, T.J.R., [1980], "Generalization of Selective Integration Procedures to Anisotropic and Nonlinear Media," *International Journal for Numerical Methods in Engineering*, Vol. 15, pp. 1413-1418.

Hughes, T.J.R, [1987], *The Finite Element Method.* Prentice-Hall, Inc., Englewood Cliffs: New Jersey.

MacNeal, R.H., [1987], "A Theorem Regarding the Locking of Tapered Four-Noded Membrane Elements," *International Journal for Numerical Methods in Engineering*, Vol. 24. pp. 1793-1799.

MacNeal, R.H. & R.L. Harder, [1985], "A Proposed Standard Set of Problems to Test Finite Element Accuracy," *Finite Elements in Analysis and Design,* Vol. 1, pp. 3-20.

Malkus, D.S. & T.J.R. Hughes, [1978], "Mixed Finite Element Methods - Reduced and Selective Integration Techniques: A Unification of Concepts," *Computer Methods in Applied Mechanics and Engineering,* Vol. 15, No. 1, pp. 63-81.

Pian, T.H.H. & K. Sumihara, [1984], "Rational Approach for Assumed Stress Finite Elements," *International Journal for Numerical Methods in Engineering,* Vol. 20, pp. 1685-1695.

Pian, T.H.H. & C.-C. Wu, [1988], "A Rational Approach for Choosing Stress Terms for Hybrid Finite Element Formulations," *International Journal for Numerical Methods in Engineering,* Vol. 26, pp. 2331-2343.

Savin, G.N., [1961], "Stress Concentration Around Holes," *International Series of Monographs in Aeronautics and Astronautics,* Pergamon Press.

Simo, J.C. & M.S. Rifai, [1989], "A Class of Mixed Assumed Strain Methods and the Method of Incompatible Modes," to appear.

Simo, J.C., R.L. Taylor & K.S. Pister, [1985], "Variational and Projection Methods for the Volume Constraint in Finite Deformation Elasto-Plasticity," *Computer Methods in Applied Mechanics and Engineering,* Vol. 51, pp. 177-208.

Strang, G. & G.J. Fix, [1973], *An Analysis of the Finite Element Method,* Prentice-Hall, Inc., Englewood Cliffs, New Jersey.

Taylor, R.L., P.J. Beresford, & E.L. Wilson, [1976], "A Nonconforming Element for Stress Analysis," *International Journal for Numerical Methods in Engineering,* Vol. 10, pp. 1211-1219.

Taylor R.L., O.C. Zienkiewicz, J.C. Simo & A.H.C. Chan, [1986], "The Patch Test for Mixed Formulations," *International Journal for Numerical Methods in Engineering,* Vol. 22, pp. 32-62.

Weissman, S.L. & Robert L. Taylor, [1990], "Treatment of Internal Constraints By Mixed Finite Element Methods: Unification of Concepts," Report No. UCB/SEMM 90/05.

Wilson, E.L., R.L. Taylor, W.P. Doherty & J. Ghaboussi, [1973], "Incompatible Displacement Modes," *Numerical and Computer Models in Structural Mechanics,* Editors S.J. Fenves, N. Perrone, A.R. Robinston & W.C. Schnobrich. Academic Press, New York.

Wu, C.-C., M.-G. Huang & T.H.H. Pian, [1987], "Consistency Condition and Convergence Criteria of Incompatible Elements: General Formulation of Incompatible Functions and its Application," *Computers & Structures*, Vol. 27, No. 5, pp. 639-644.

Zienkiewicz, O.C., S. Qu, R.L. Taylor & S. Nakazawa, [1986], "The Patch Test for Mixed Formulations," *International Journal for Numerical Methods in Engineering*, Vol. 23, pp. 1873-1883.

Zienkiewicz, O.C. & R.L. Taylor, [1989], *The Finite Element Method*, 4th edition, MacGraw-Hill Book Co., London.

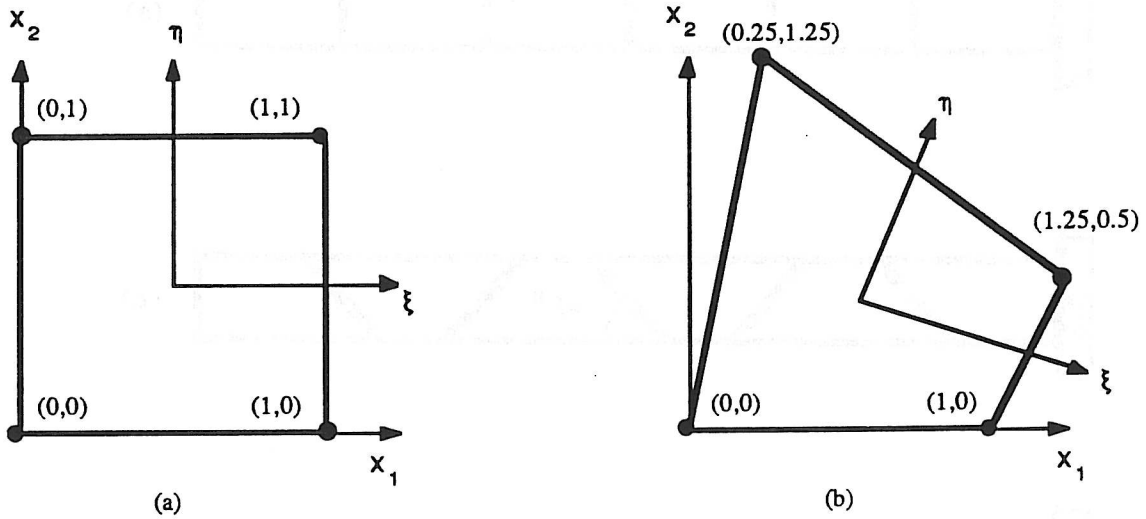

Figure 5.1: (a) Square element; (b) Element distorted from a parallelogram shape.

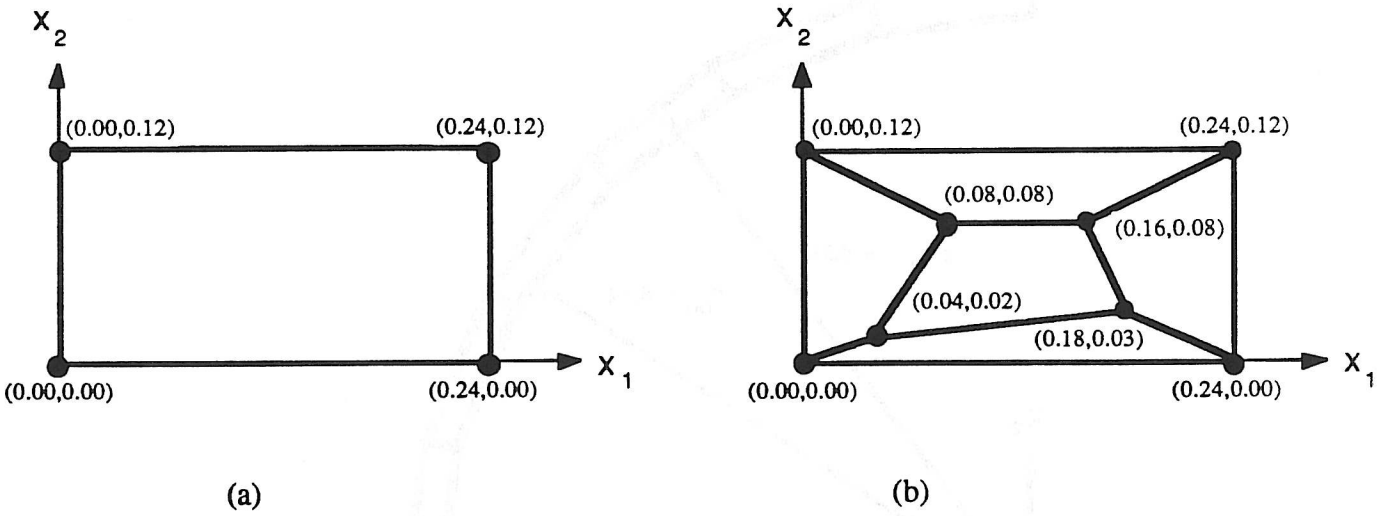

Figure 6.1: Patch test - (a) One-element mesh, (b) Skewed mesh.

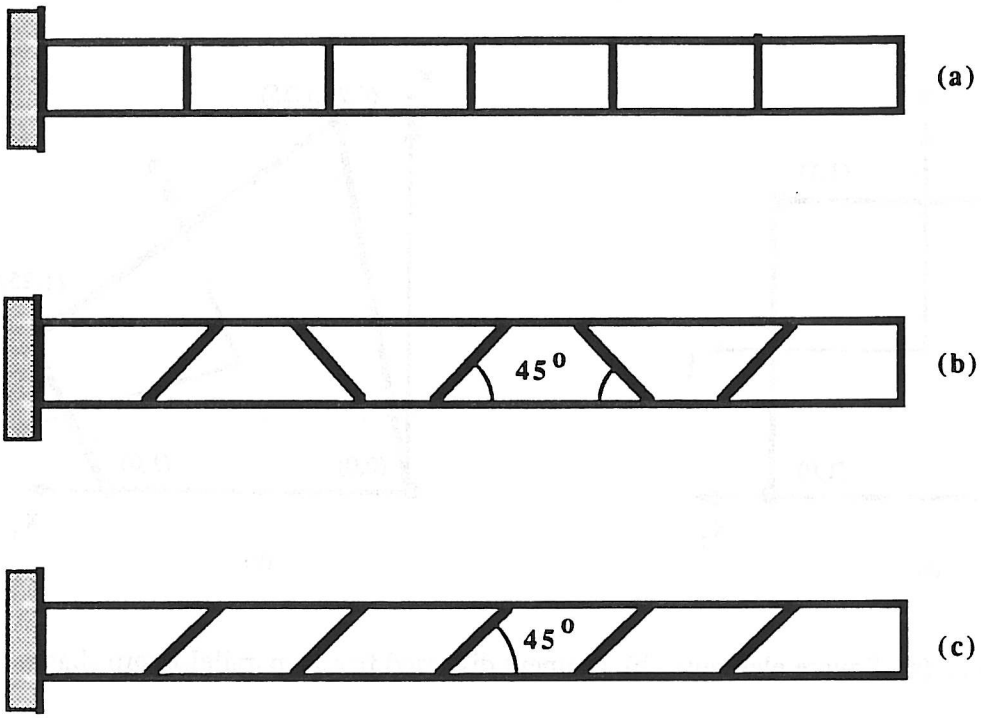

Figure 6.2: Straight cantilever beam. (a) Regular shape elements; (b) Trapezoid shape elements; (c) Parallelogram shape elements.

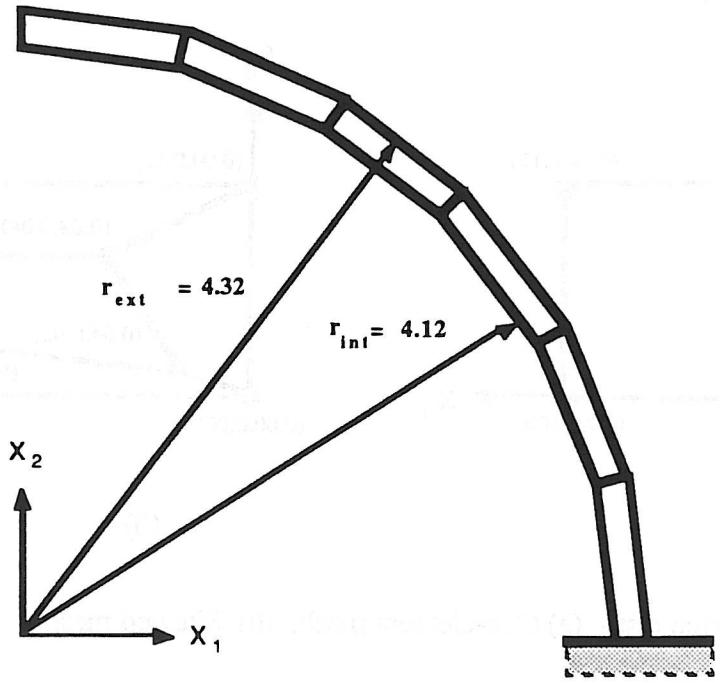

Figure 6.3: Curved beam mesh.

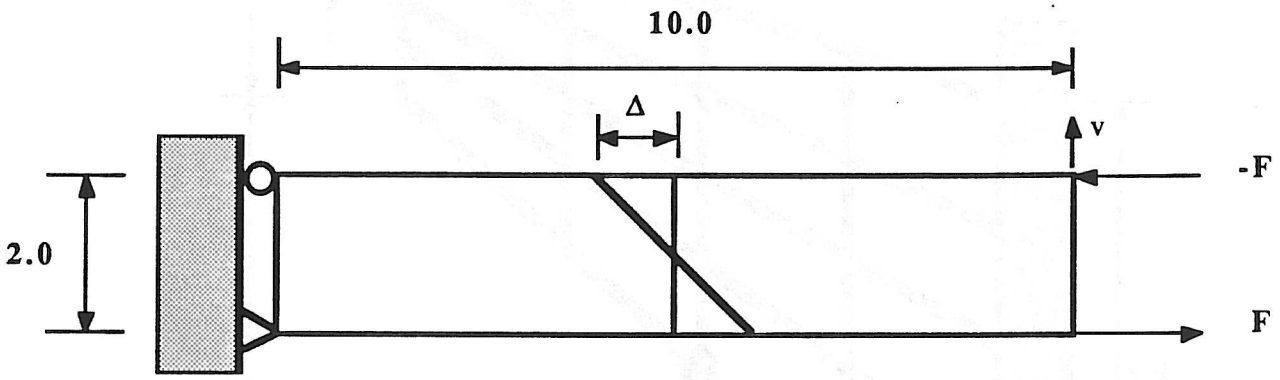

Figure 6.4: Beam bending problem, sensitivity to mesh distortion.

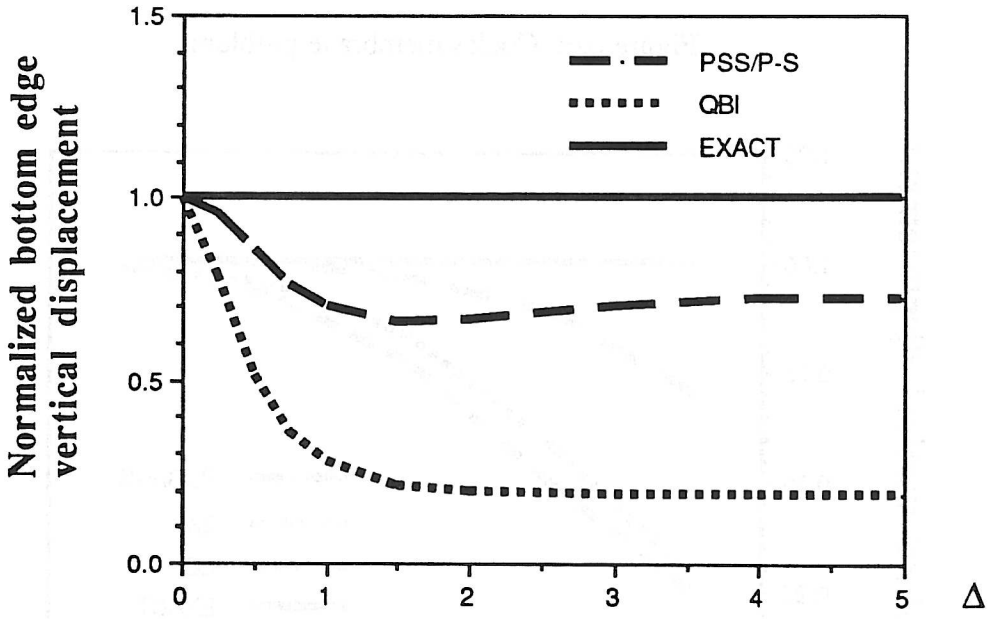

Figure 6.5: Beam bending, sensitivity to mesh distortion: normalized tip displacement.

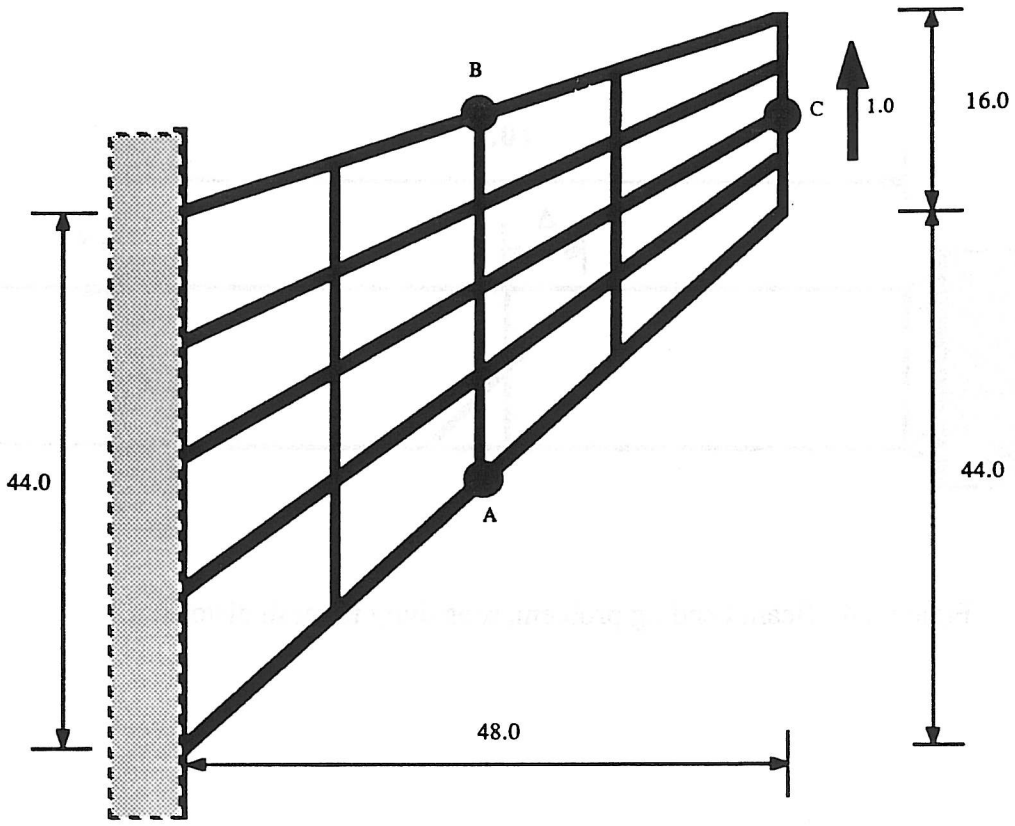

Figure 6.6: Cook's membrane problem.

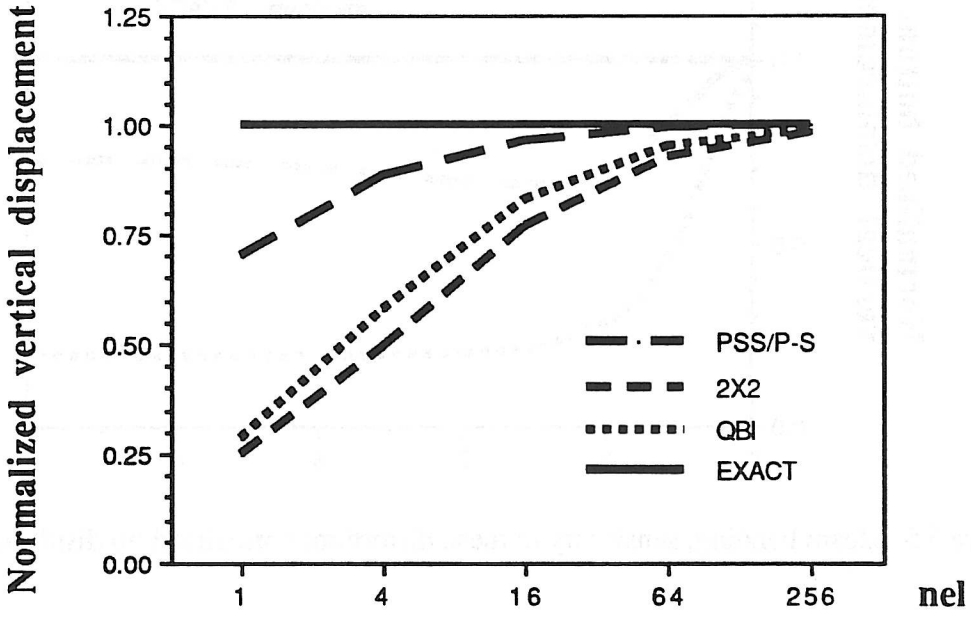

Figure 6.7: Cook's membrane problem; vertical displacement at point C.

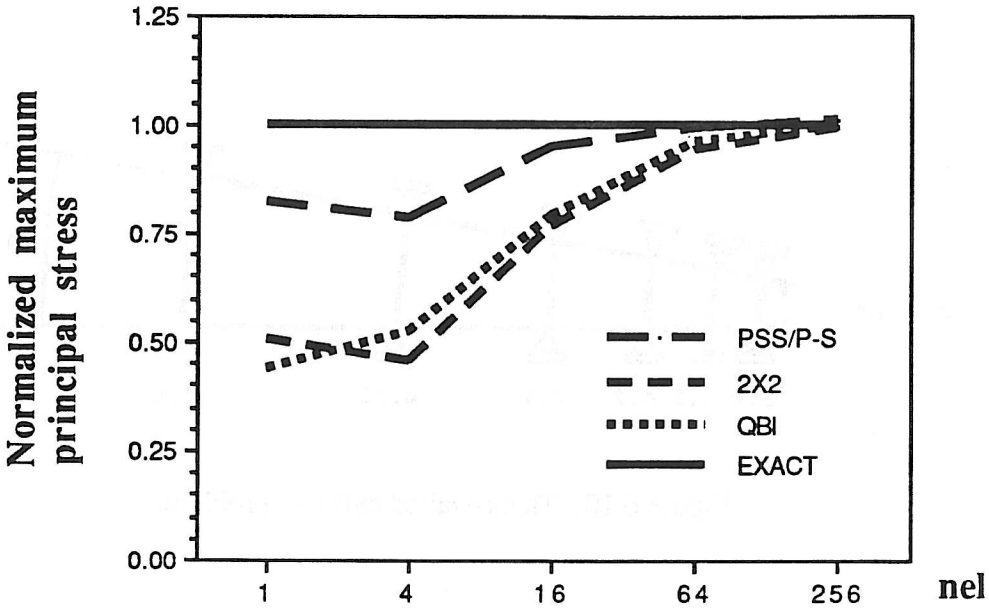

Figure 6.8: Cook's membrane problem; maximum principal stress at point A.

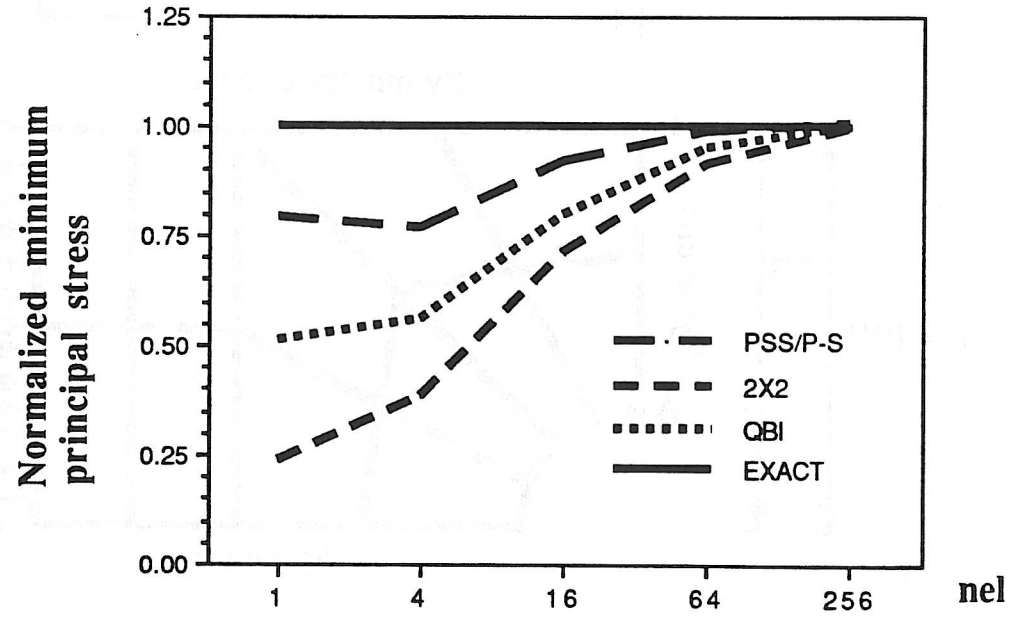

Figure 6.9: Cook's membrane problem; minimum principal stress at point B.

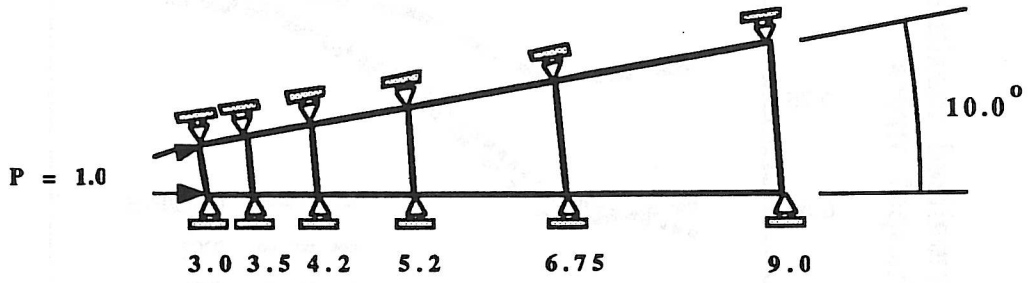

Figure 6.10: Thick-walled cylinder problem.

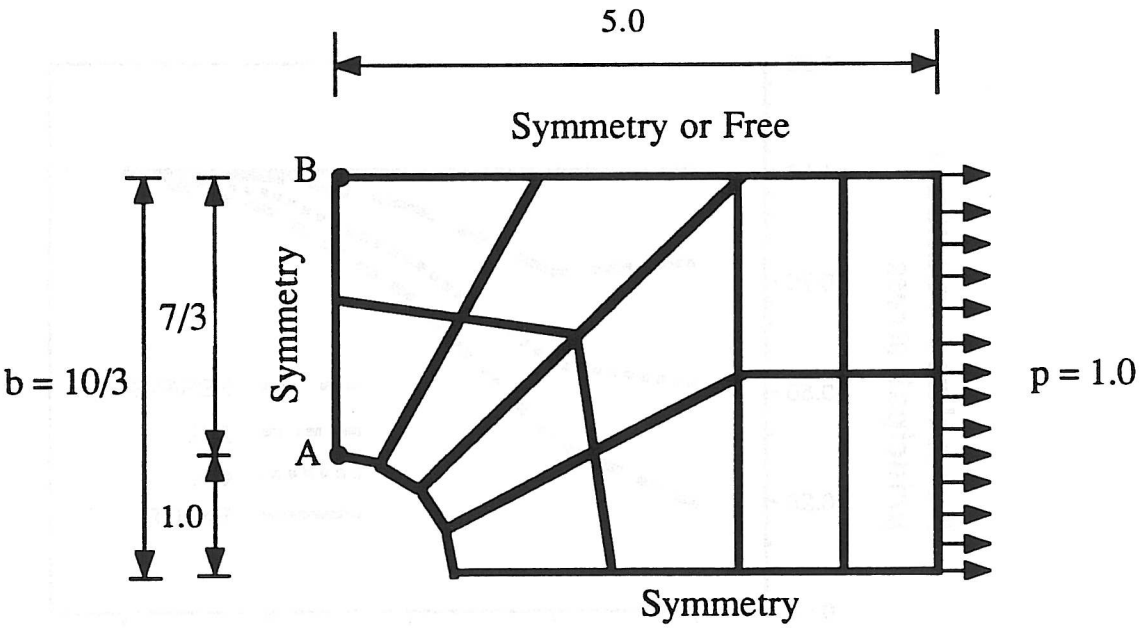

Figure 6.11: Strip with a hole problem.

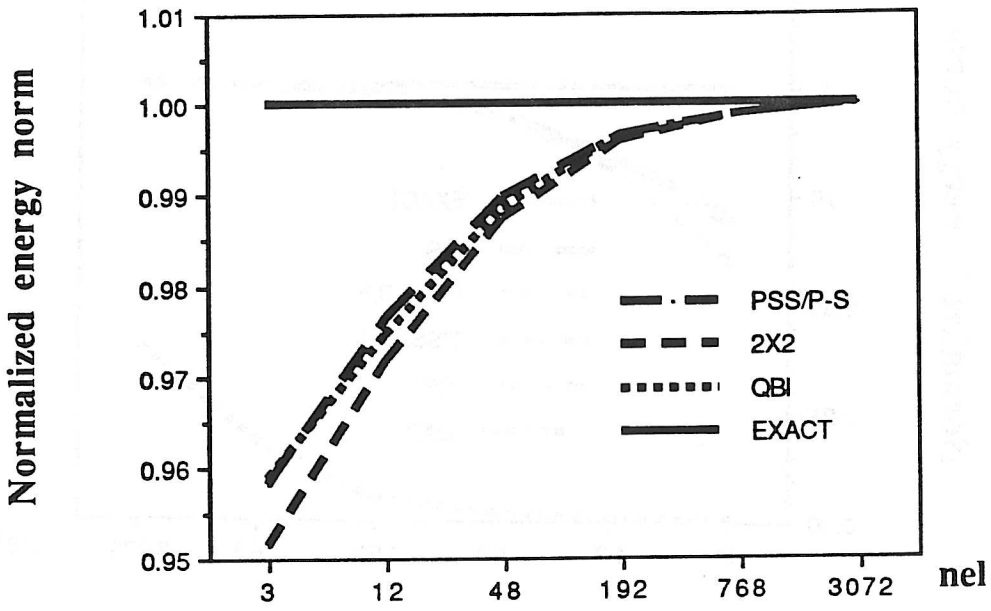

Figure 6.12: Strip with a hole; plane stress; convergence in the energy norm.

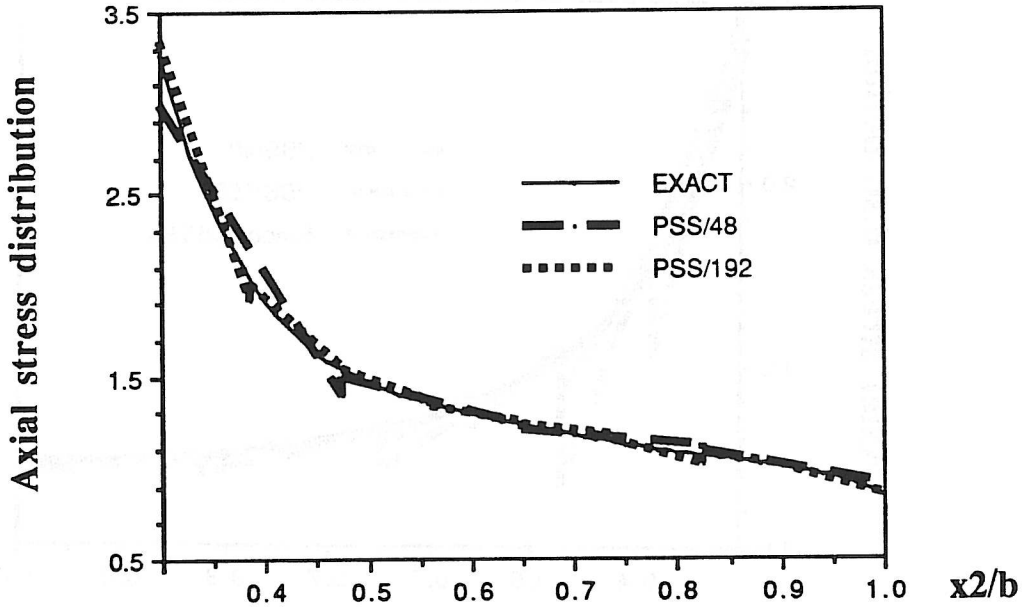

Figure 6.13: Strip with a hole; plane stress; axial stress distribution along the line A-B.

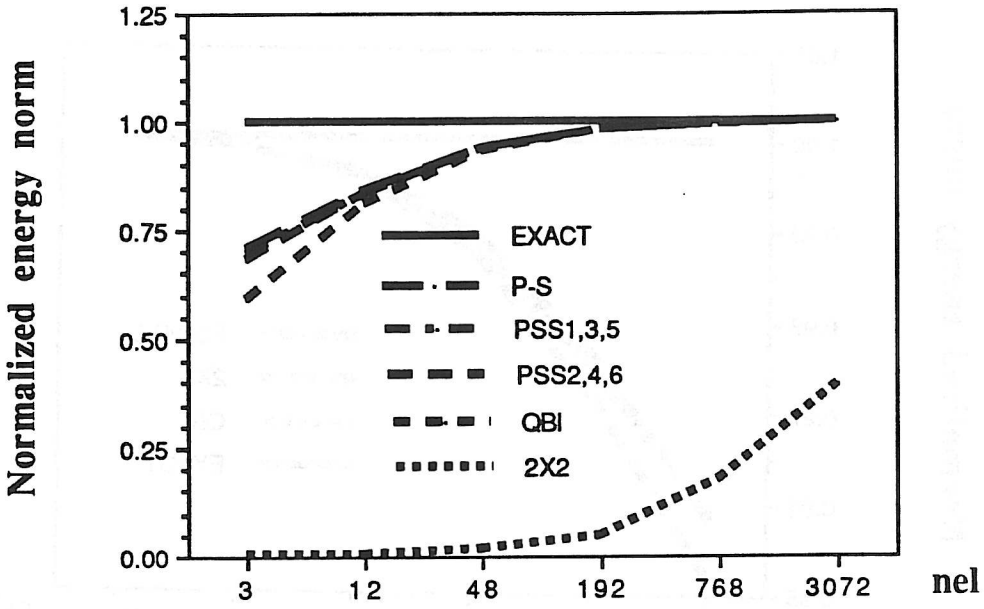

Figure 6.14: Strip with a hole; plane strain; convergence in the energy norm.

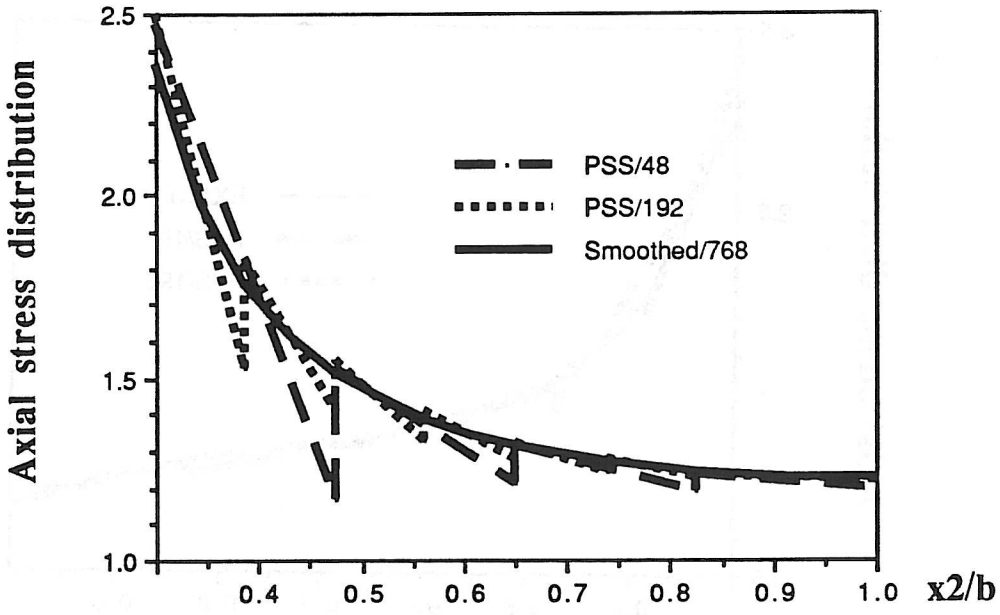

Figure 6.15: Strip with a hole; plane strain; axial stress distribution along the line A-B.